European Journal of Medicinal Chemistry 62 (2013) 199–205

Contents lists available at SciVerse ScienceDirect

European Journal of Medicinal Chemistry

journal homepage: http://www.elsevier.com/locate/ejmech

Short communication

# Novel agmatine dipeptide inhibitors against the West Nile virus NS2B/NS3 protease: A P3 and N-cap optimization study

Huichang Annie Lim, Melgious Jin Yan Ang, Joma Joy, Anders Poulsen, Wenshi Wu, Shi Chie Ching, Jeffrey Hill, Cheng San Brian Chia*

*Experimental Therapeutics Centre, Agency for Science, Technology and Research (A*STAR), 31 Biopolis Way, Nanos #03-01, Singapore 138669, Singapore*

ARTICLE INFO

*Article history:*
Received 11 October 2012
Received in revised form
11 December 2012
Accepted 25 December 2012
Available online 3 January 2013

*Keywords:*
Agmatine
Peptide
West Nile virus
NS2B/NS3
Serine protease inhibitor

ABSTRACT

This communication describes the synthesis and inhibitory activities of thirty-seven novel C-terminal agmatine dipeptides used as screening compounds to study the structure–activity relationship between active-site peptidomimetics and the West Nile virus (WNV) NS2B/NS3 serine protease. Our efforts lead to the discovery of a novel agmatine dipeptide inhibitor (compound **33**, $IC_{50}$ 2.6 ± 0.3 μM) with improved inhibitory activity in comparison to the most potent inhibitor described in our recent report [$IC_{50}$ 4.7 ± 1.2 μM; Lim et al., Eur. J. Med. Chem. 46 (2011) 3130–3134]. In addition, our study cleared the contention surrounding the previous X-ray co-crystallization study and an enzyme inhibition report on the binding conformation adopted by active-site peptide aldehydes. Our data should provide valuable insights into the design of future peptidomimetic antivirals against WNV infections.



## 1. Introduction

The West Nile virus (WNV) is a member of the *Flaviviridae* family of viruses transmitted by *Culex* mosquitoes [1]. Originating from Africa, it has spread to humans in Asia, southern Europe, the Middle East and North America [2,3]. Symptoms of infection include fever, headaches, chills, diaphoresis, enlarged lymph nodes and arthralgia [4]. Approximately 60% of these cases progress to encephalitis with a fatality rate of 10% [1]. Between 1999 and 2011, the United States Center for Disease Control reported more than 23,000 human infections in North America, resulting in 1251 deaths [5]. More recently, an outbreak occurred in North America, with 1118 human infections and 41 fatalities [6]. There is currently no vaccine or specific drug therapy to treat WNV infections, thus creating an urgent need to develop a drug against this disease [7].

The WNV has a single-strand, 11-kb RNA genome which acts as a messenger RNA for protein synthesis and a template for RNA replication in mammalian host cells. The viral genome encodes seven nonstructural proteins (NS1, NS2A, NS2B, NS3, NS4A, NS4B and NS5) [8]. NS3 complexes with its co-factor NS2B to form a serine protease in the host cell which hydrolyze polyprotein precursors into functional proteins responsible for viral replication [9]. This trypsin-like protease is specific for protein substrates containing two consecutive basic residues (Lys-Arg) at the P2 and P1 positions respectively, cleaving the C-terminal end of arginine (Fig. 1A) [10,11]. This unusual specificity is not found in many mammalian proteases, making NS2B/NS3 a potential drug target [12–14].

In 2008, a cell permeable, serum stable, non-cytotoxic tripeptide aldehyde inhibitor (Lys-Lys-Arg-H) was demonstrated to competitively inhibit the WNV NS2B/NS3 protease at nanomolar potency, bringing the field a step closer to the development of the first WNV drug [15]. A year later, the X-ray crystal structure of the WNV NS2B/NS3 protease complexed to the tripeptide aldehyde inhibitor, 2-naphthoyl-Lys-Lys-Arg-H, was solved [16]. The naphthoyl N-terminal capping group (N-cap) was observed to be solvent-exposed and did not interact with the protease (Fig. 1B). Intriguingly, modifications to the N-cap drastically affected inhibitory activities, with up to 30-fold differences in $IC_{50}$ values [15]. The authors attributed these conflicting observations to artifacts of crystallization and using molecular dynamics and simulated annealing calculations, proposed alternative ligand binding poses with the N-cap binding to the protease S4 subsite [15].

Recently, we showed that agmatine dipeptide **1** (Fig. 2) could competitively inhibit the WNV NS2B/NS3 protease with an $IC_{50}$ of 4.7 ± 1.2 μM [17]. Peptides containing a P1 agmatine at their

* Corresponding author. Tel.: +65 64070348; fax: +65 64788768.
*E-mail address:* cschia@etc.a-star.edu.sg (C.S.B. Chia).

0223-5234/$ – see front matter © 2013 Elsevier Masson SAS. All rights reserved.
http://dx.doi.org/10.1016/j.ejmech.2012.12.043

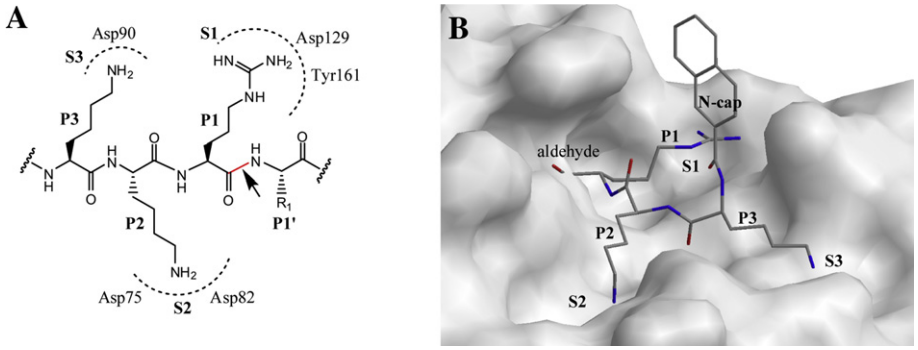


**Fig. 1.** (A) Schematic diagram of a peptide substrate showing the scissile bond (arrowed) and P1–P3 residues using conventional terminology [11]. Protease residues involved in substrate binding are numbered based on the crystal structure 3E90.pdb. (B) Co-crystal structure (3E90.pdb) of naphthoyl-KKR-H (stick model) bound to the WNV NS2B/NS3 protease.

C-termini have been shown to inhibit various serine proteases, including thrombin and furin [18,19]. These peptidomimetics resemble peptide aldehydes without the reactive C-terminal aldehyde functionality. Although less potent, they do not cyclize in solution and can be easily and rapidly synthesized using solid-phase chemistry [20], making them ideal tool compounds for studying enzyme–inhibitor interactions. To gain better insights into the conflicting X-ray and enzyme inhibition data, we conducted a structure–activity relationship (SAR) study using thirty-seven novel agmatine dipeptide NS2B/NS3 inhibitors with various P3 and N-cap analogs. We believe our findings will be invaluable to medicinal chemists involved in the design and development of novel WNV protease inhibitors.

## 2. Results and discussion

### 2.1. Chemistry

The preparation of compound **1** can be found in a previous report [17]. The synthetic procedure for the remaining compounds was published recently [20] and is outlined in Scheme 1. Detailed synthetic procedures are reported in the supplementary notes.

### 2.2. Biological activity

Inhibitory activities of the agmatine dipeptides are summarized in Table 1. Compound **1** was modeled using the WNV NS2B/NS3 crystal structure 3E90.pdb complexed to the tripeptide aldehyde inhibitor (2-naphthoyl-KKR-H) as a template. Structural analysis revealed that the inhibitor adopted a 'C'-shaped conformation with

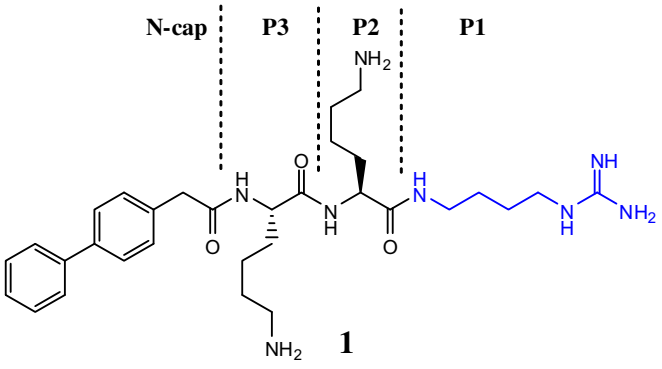


**Fig. 2.** Structure of compound **1** linked to an agmatine moiety (in blue) and demarcated into four regions (P1, P2, P3 and N-cap). (For interpretation of the references to colour in this figure legend, the reader is referred to the web version of this article.)

the guanidino $N^{\varepsilon}$ involved in intra-molecular hydrogen bonding to the carbonyl O of the 4-phenyl-phenacetyl (4-PhPhac) N-cap (Fig. 3A). To probe the binding role of the P3 residue, we synthesized compound **2** (Table 1) and discovered that a single residue truncation abrogated its inhibitory activity ($IC_{50} > 100$ μM), suggesting that the P3 Lys played an important enzyme inhibitory role. Changing the stereochemistry of P3 Lys to its D enantiomer (compound **3**) also resulted in a loss of activity ($IC_{50} > 100$ μM; Table 1), suggesting that the ligand–protease binding was stereospecific.

Substituting the P3 Lys with non-polar (compounds **4**–**9**), uncharged polar (compounds **10**–**12**) and anionic residues (compounds **13** and **14**) resulted in either a total loss or drastic reduction in inhibitory activities, highlighting the specificity of the S3 binding pocket (Table 1). Interestingly, compound **8** with a P3 norleucine (Nle) retained some inhibitory activity ($IC_{50}$ 47.9 ± 6.2 μM). This may be because Nle is an analog of Lys without the cationic $N^{\varepsilon}$ amino group, suggesting that the amino moiety played an important binding role within the S3 subsite (Fig. 3A). Intrigue by this, we substituted the P3 Lys with another cationic residue, arginine (compound **15**). Assay results revealed that compound **15** suffered a 4-fold decrease in inhibitory activity compared to **1** ($IC_{50}$ 19.1 ± 2.0 vs. 4.7 ± 1.2 μM; Table 1), suggesting that the enzyme's S3 binding pocket was lysine specific. Modeling revealed that the more bulky arginine side chain was too bulky to fit completely into the S3 subsite due to steric interactions caused by Gln86 and Met156 and the guanidino moiety could not make the same hydrogen bond interactions like the $N^{\varepsilon}$ amino group of the P3 lysine (Fig. 3B).

Next, the P3 Lys was replaced with aromatic residues (compounds **16**–**18**). Compound **16** with a P3 His showed no inhibitory activity while compounds **17** and **18** displayed weak inhibitory activities ($IC_{50}$ 44.5 ± 5.3 and 33.5 ± 2.7 μM; Table 1). Docking studies of compound **18** revealed that the Trp indole side chain could participate in hydrophobic interaction and hydrogen bond to the Ile155 side chain and carbonyl moiety respectively (Fig. 3C). Based on the $IC_{50}$s of compounds **2**–**18**, we concluded that Lys was the optimal residue for enzyme binding and our P3 mutation results were in agreement with the co-crystal structure published by Robin and co-workers (3E90.pdb) [16].

Our next series of inhibitors involved N-cap mutation. As mentioned earlier, the carbonyl O of the N-cap was observed to be involved in intra-molecular hydrogen bonding with the P1 guanidino $N^{\varepsilon}$ moiety (~1.7 Å). This oriented the aromatic portion of the N-cap 3.6 Å away from the agmatine guanidino group (distance between the guanidino central C to the ring center) and could therefore participate in intra-molecular cation-π stacking (Fig. 3A). To investigate the role played by this intra-molecular hydrogen bond, we removed the carbonyl functionality by converting

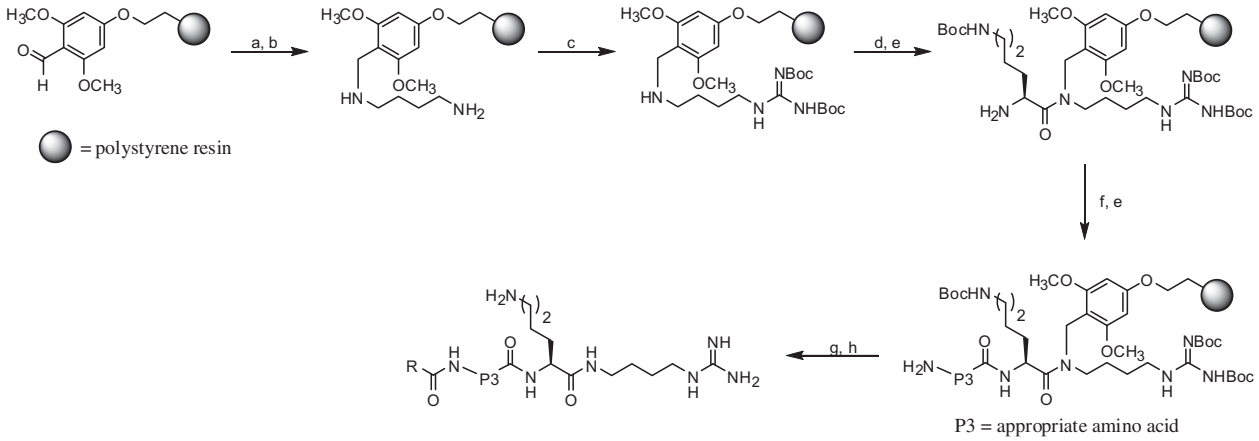


**Scheme 1.** Synthesis of agmatine dipeptides. Reagents and conditions: (a) resin swelling in DMF, 25 °C, 1 h; (b) 1,4-diaminobutane, $NaCNBH_3$, 1% AcOH in DMF (v/v), microwave, 60 °C, 10 min, repeat; (c) *N*,*N*′-bis(*tert*-butoxy carbonyl)thiourea, DIPEA, DMF, microwave, 60 °C, 10 min; (d) Fmoc-Lys(Boc)-OH, DIC, HOBt, 90% $CH_2Cl_2$ in DMF (v/v), microwave, 60 °C, 10 min, repeat; (e) 20% piperidine in DMF (v/v), microwave, 60 °C, 5 min; (f) Fmoc-P3-OH, DIC, HOBt, 90% $CH_2Cl_2$ in DMF (v/v), microwave, 60 °C, 10 min; (g) Appropriate carboxylic acid, DIC, HOBt, 90% $CH_2Cl_2$ in DMF (v/v), microwave, 60 °C, 10 min; (h) 95% TFA in $CH_2Cl_2$ (v/v), 25 °C, 30 min.

the N-terminus into a free amine (compound **19**; Table 1). Experimental results were striking, showing an 8-fold decrease in inhibitory activity compared to compound **1** ($IC_{50}$ 38.2 ± 5.7 vs 4.7 ± 1.2 μM). A plausible explanation could be that the cationic guanidino moiety was repulsed by the positively-charged N-terminus, resulting in an increase in conformational energy and a decrease in binding affinity. This supports the 'C'-shaped binding pose adopted by 2-naphthoyl-KKR-H in the X-ray co-crystal structure [16]. Replacing the biphenyl moiety with non-aromatic alkyl groups should also abrogate inhibitory potencies by removing the cation-π stacking. To test this hypothesis, the 4-PhPhac N-cap was replaced with six alkyl moieties (compounds **20**–**25**). Starting with an acetyl capping group (compound **20**), an approximate 4-fold reduction in inhibitory activity was observed compared to compound **1** ($IC_{50}$ 18.2 ± 2.5 vs 4.7 ± 1.2 μM), supporting our hypothesis. Computer modeling revealed that the methyl group of the acetyl N-cap could participate in hydrophobic interaction with the protease Ile155 side chain (Fig. 3D). Lengthening the acetyl with propanoyl, butanoyl and 3-methylbutanoyl groups did not significantly affect inhibitory activities (compounds **21**–**23**; Table 1). However, substituting them for branched acyl moieties caused a slight reduction in activities (compounds **24** and **25**; Table 1). Modeling of compound **25** with a trimethylacetyl N-cap suggested that this could be due to steric hindrance between the bulky trimethylacetyl group and the protease Ile155 side chain (Fig. 3E).

Next, we substituted the N-caps with aromatic benzoyl and naphthoyl moieties (compounds **26**–**28**; Table 1). Surprisingly, their inhibitory activities were approximately 2-fold less potent than the acetyl analog (compound **20**). Modeling of compound **27** showed that the aromatic N-cap was largely solvent-exposed (Fig. 3F) and the observed reduction in activity could be due to its structural rigidity which prevented the naphthoyl group from orienting itself into a more favorable position for hydrophobic interactions with Ile155.

Further examination of the docked model of compound **1** revealed that its 4-PhPhac N-cap was situated between two 'cliffs' formed by Thr132 and Ile155 of the enzyme (Fig. 3A). The phenyl ring distal to the N-cap carbonyl could take part in hydrophobic interaction with the enzyme's Pro131 five-membered ring. To investigate further, we replaced the 4-PhPhac with a phenacetyl (Phac) group (compound **29**; Table 1). Protease inhibition results revealed an approximate 2-fold decrease in activity compared to compound **1** ($IC_{50}$ 8.5 ± 0.9 vs 4.7 ± 1.2 μM; Table 1), suggesting that the distal phenyl ring of 4-PhPhac was also involved in enzyme binding. Next, we investigated the binding role of the N-cap Phac group of compound **29**. As observed earlier, the aromatic ring was situated ~3.6 Å from the P1 guanidino moiety (distance between the ring center to the central guanidino C), allowing favorable intramolecular cation-π stacking to occur. Substituting Phac with 3-phenylpropanoyl and 4-phenylbutanoyl functionalities (compounds **30** and **31**; Table 1) should disrupt the cation–π interactions and hence reduce their inhibitory activities. As expected, compound **30** exhibited a 5-fold decrease in activity compared to compound **29** ($IC_{50}$ 42.2 ± 6.0 vs. 8.5 ± 0.9 μM) while compound **31** displayed only a slight reduction in potency ($IC_{50}$ 11.2 ± 1.0 μM; Table 1). Intrigued, we modeled compounds **30** and **31** into the protease followed by energy minimization. Results showed that the phenyl ring of compound **30** was situated ~4.1 Å away from the P1 guanidino moiety (measured from the ring center to the central C of the guanidino group), compared to 3.6 Å for compound **29**. This could have reduced intra-molecular cation–π interactions with the P1 guanidino moiety (Fig. 3G). For compound **31**, the propylene chain shifted the phenyl ring away from the P1 guanidino moiety and oriented it 3.8 Å toward the NH of Thr132 (Fig. 3H). As aromatic rings can act as hydrogen bond acceptors, this could have resulted in favorable dipole–π interactions and may explain why compound **31** was 4-fold more potent than **30** ($IC_{50}$ 11.2 ± 1.0 vs. 42.2 ± 6.0 μM; Table 1).

In the last series of inhibitors, ring-substitution studies were conducted on the N-cap Phac group. Shifting the 4-phenyl ring of compound **1** to the 3-position (compound **32**; Table 1) resulted in a 2-fold decrease in inhibitory activity ($IC_{50}$ 4.7 ± 1.2 vs. 9.9 ± 2.3 μM; Table 1). This may be due to loss of the hydrophobic interaction between the phenyl ring and the enzyme's Pro131 ring (Fig. 3I). Placing a Cl moiety at the 2-, 3- and 4-positions of the N-cap Phac (compounds **33**–**35**; Table 1) yielded different inhibitory results. The most potent inhibitor, compound **33**, with a 2-Cl substituent was 2-fold more potent than compound **1** ($IC_{50}$ 2.6 ± 0.3 vs. 4.7 ± 1.2 μM respectively; Table 1). Our molecular model suggested that the 2-Cl group could either participate in dipole–dipole interaction with the side chain hydroxyl of Thr132 or have increased hydrophobic interactions with Ile155 (Fig. 3J). The 3-Cl analog (compound **34**; $IC_{50}$ 9.6 ± 2.0 μM), like compound **32**, was likely to be sterically hindered if pointing toward Thr132 and is hence likely to point in the opposite direction (Fig. 3K). This was likely to orient the 3-Cl moiety too far to interact with Thr132.

**Table 1**
Inhibitory data of agmatine dipeptide inhibitors with the sequence: (N-cap)-P3-Lys-agmatine.

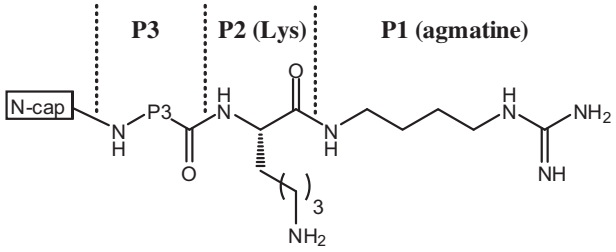


| Compound | N-cap | P3 | $IC_{50}$ (μM) |
|---|---|---|---|
| **1** | 4-PhPhac | Lys | 4.7 ± 1.2 |
| **2** | – | $CH_3$ (acetyl) | >100 |
| **3** | 4-PhPhac | D-Lys | >100 |
| **4** | 4-PhPhac | Gly | >100 |
| **5** | 4-PhPhac | Ala | 53.7 ± 6.8 |
| **6** | 4-PhPhac | Val | >100 |
| **7** | 4-PhPhac | Leu | >100 |
| **8** | 4-PhPhac | Nle | 47.9 ± 6.2 |
| **9** | 4-PhPhac | Pro | >100 |
| **10** | 4-PhPhac | Asn | >100 |
| **11** | 4-PhPhac | Gln | >100 |
| **12** | 4-PhPhac | Ser | >100 |
| **13** | 4-PhPhac | Asp | >100 |
| **14** | 4-PhPhac | Glu | >100 |
| **15** | 4-PhPhac | Arg | 19.1 ± 2.0 |
| **16** | 4-PhPhac | His | >100 |
| **17** | 4-PhPhac | Phe | 44.5 ± 5.3 |
| **18** | 4-PhPhac | Trp | 33.5 ± 2.7 |
| **19** | H | Lys | 38.2 ± 5.7 |
| **20** |  | Lys | 18.2 ± 2.5 |
| **21** | 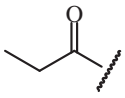 | Lys | 19.1 ± 3.3 |
| **22** | 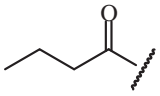 | Lys | 18.5 ± 4.1 |
| **23** | 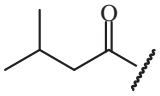 | Lys | 19.2 ± 4.2 |
| **24** | 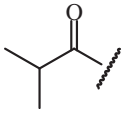 | Lys | 23.8 ± 4.8 |
| **25** | 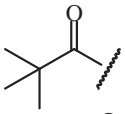 | Lys | 27.1 ± 5.0 |
| **26** | 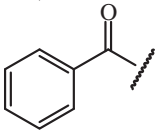 | Lys | 38.6 ± 5.3 |
| **27** | 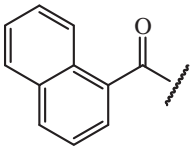 | Lys | 33.3 ± 3.9 |

**Table 1** (*continued*)

| Compound | N-cap | P3 | $IC_{50}$ (μM) |
|---|---|---|---|
| **28** | 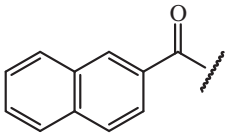 | Lys | 32.5 ± 4.7 |
| **29** | 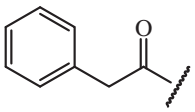 | Lys | 8.5 ± 0.9 |
| **30** | 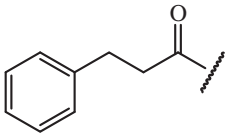 | Lys | 42.2 ± 6.0 |
| **31** | 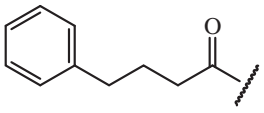 | Lys | 11.2 ± 1.0 |
| **32** | 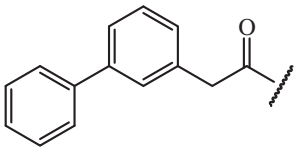 | Lys | 9.9 ± 2.3 |
| **33** | 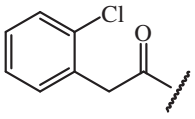 | Lys | 2.6 ± 0.3 |
| **34** | 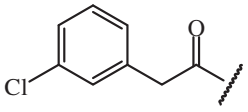 | Lys | 9.6 ± 2.0 |
| **35** | 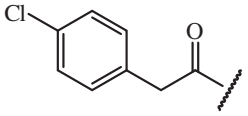 | Lys | 4.8 ± 1.0 |
| **36** | 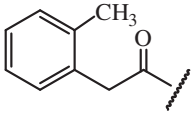 | Lys | 6.8 ± 1.2 |
| **37** | 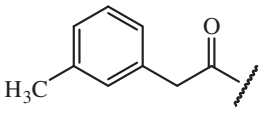 | Lys | 9.2 ± 1.6 |
| **38** | 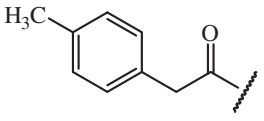 | Lys | 6.9 ± 1.3 |

Unsurprisingly, compounds **32** and **34** exhibited almost identical inhibitory potencies ($IC_{50}$ 9.9 ± 2.3 vs. 9.6 ± 2.0 μM respectively). Similarly, compound **35** with a 4-Cl moiety also exhibited identical potency to compound **1** ($IC_{50}$ 4.8 ± 1.0 vs. 4.7 ± 1.2 μM respectively), suggesting that the 4-phenyl ring could be replaced with 4-Cl moiety (Fig. 3L). The 4-Cl was too far to interact with the hydroxyl group of Thr132 or the side chain of Ile155 unlike compound **33** and this may account for its weaker $IC_{50}$ (4.8 ± 1.0 vs. 2.6 ± 0.3 μM respectively). Substituting Cl with a methyl group at

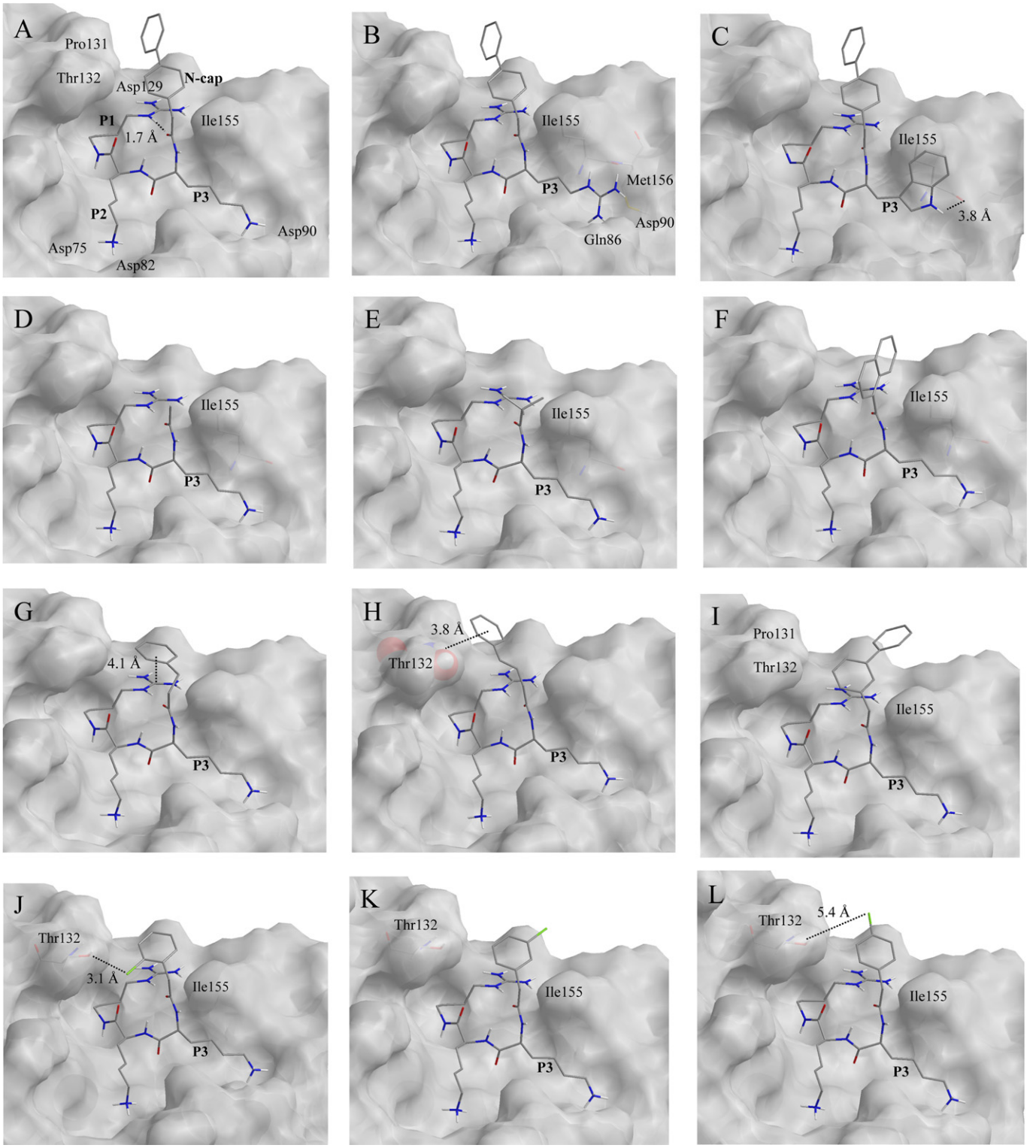


**Fig. 3.** Stick models of selected compounds docked onto the WNV NS2B/NS3 catalytic site using 3E90.pdb as a template; (A) Cpd. **1**; (B) Cpd. **15** showing steric hindrance caused by Gln86 and Met156; (C) Cpd. **18** showing interactions between P2 Trp and Ile155; (D) Cpd. **20** showing the proximity of the acetyl N-cap to Ile155; (E) Cpd. **25** showing steric clash between its N-cap with Ile155; (F) Cpd. **27** with its solvent-exposed N-cap; (G) Cpd. **30** showing possible intra-molecular cation–π interactions between the N-cap and the P1 guanidino moiety; (H) Cpd. **31** N-cap interacting with Thr132 NH (CPK model); (I) Cpd. **32** with its N-cap oriented between Thr132 and Ile155; (J) Cpd. **33** showing its 2-Cl N-cap interacting with Thr132; (K) Cpd. **34** with its 3-Cl N-cap between Thr132 and Ile155; (L) Cpd. **35** with its 4-Cl N-cap too far away to interact with Thr132.

the 2-, 3- and 4-positions (compounds **36**–**38**; Table 1) yielded a similar pattern of results albeit at reduced potencies. For example, replacing the 2-Cl (compound **33**) with 2-methyl (compound **36**) resulted in an approximate 3-fold reduction in inhibitory activity ($IC_{50}$ 2.6 ± 0.3 vs. 6.8 ± 1.2 μM respectively). A possible explanation may be due to the loss in dipole–dipole interaction with the side chain hydroxyl of Thr132 when 2-Cl is replaced with a methyl group (Fig. 3J). Interestingly, replacing 3-Cl (compound **34**) with

3-methyl (compound **37**) did not result in significant changes in activity ($IC_{50}$ 9.6 ± 2.0 vs. 9.2 ± 1.6 μM respectively). This was probably because ring substituents at the *meta* position could not interact with the protease (see Fig. 3I and K). The final analog tested, compound **38**, exhibited a slight reduction in activity compared to compound **1** ($IC_{50}$ 6.9 ± 1.3 vs. 4.7 ± 1.2 μM respectively). A plausible explanation could be that replacing the 4-phenyl group with a methyl could have reduced the hydrophobic interaction between the 4-Ph and Pro131.

## 3. Conclusion

In this communication, we demonstrated that agmatine dipeptides can be utilized as tool compounds for SAR studies on ligand–enzyme interactions. We were able to confirm that the optimal P3 residue for enzyme inhibition was Lys, supporting an earlier screening effort involving a small tripeptide aldehyde library [21]. Our data also support both the proposed X-ray co-crystal structure published by Robin and co-workers (3E90.pdb) [16] and the peptide aldehyde enzyme inhibition data [15]. In the former, we believe the inhibitor N-cap did not interact directly with the protease (Fig. 1B) and was not due to an artifact of crystallization. The seemingly conflicting conclusions based on the two papers [15,16] were possibly due to inadequate SAR studies on the inhibitor N-cap. Based on our experimental results, we conclude that certain N-caps indeed have minimal interaction with the protease (as in the cases shown in Figs. 1B and 3F), while some N-caps could orient themselves favorably to interact with the protease as exemplified by compound **33** (Fig. 3J). Finally, by synthesizing and screening thirty-seven analogs of compound **1**, we were able to identify a novel agmatine dipeptide with a two-fold improvement in inhibitory activity (compound **33**). Taken together, our data should provide medicinal chemists with deeper insights into the design of new drugs for the treatment of WNV infections.

## 4. Experimental protocols

### 4.1. Chemistry

All reagents and solvents were obtained from commercial sources and were used without further purification. Acetonitrile was purchased from Merck KGaA (Germany). Fmoc-protected amino acids and HBTU were bought from GL Biochem (China). $CD_3OD$ was purchased from Cambridge Isotope Laboratories (USA). All other reagents were purchased from Sigma–Aldrich (USA). Crude target inhibitors were purified using a reverse-phase C18 column (Waters X-bridge) on a high performance liquid chromatography (HPLC) system with an ultraviolet detector set at 215 nm (Shimadzu Prominence). The mobile phase consisted of solvent A (water) and solvent B (acetonitrile). The gradient started with 1% solvent B for 5 min which was increased to 11% in 40 min. All target compounds were characterized by electrospray ionization-time of flight-mass spectrometry (ESI-TOF-MS; Agilent 6224 TOF) using Mass Hunter software. NMR spectra were recorded on a Bruker Ultrashield 400+ spectrometer in $CD_3OD$. Chemical shifts were expressed as $\delta$ (ppm) relative to TMS.

#### 4.1.1. Synthesis of compounds

The preparation of compound **1** can be found in a previous report [17]. The general synthetic outline of compounds **2**–**38** is shown in Scheme 1 and is based on a previous report [20]. Synthetic details can be found in the supplementary notes. Spectral data of compound **33**: $^1$H NMR (400 MHz, $CD_3OD$) $\delta$ 1.29–1.85 (16H, m, lysine side chains), 2.80–3.23 (8H, m, agmatine), 3.78 (2H, s, Ar–$CH_2$–CO–), 4.26–4.28 (2H, m, lysine α-Hs), 7.28–7.40 (4H, m, aromatics); $^{13}$C NMR (100 MHz, $CD_3OD$) $\delta$ 23.8, 23.9, 27.0, 27.4, 28.0, 28.1, 32.0, 32.4, 39.9, 40.5, 40.6, 41.2, 48.5, 48.7, 48.9, 128.5, 130.1, 130.5, 133.2, 134.6, 135.5, 158.3, 173.7, 174.2, 174.7. ESI-TOF-MS: *m/z* calc $C_{25}H_{44}ClN_8O_3$ ($M + H^+$) 539.3225, found 539.3221.

### 4.2. Biological activities

#### 4.2.1. WNV NS2B/NS3 enzyme inhibition assay

WNV NS2B/NS3 inhibitory assays were based on published work [10] and performed in a buffer at pH 8.0 containing Tris–HCl (10 mM), CHAPS (1 mM) and glycerol (20% v/v). The enzyme (20 nM) and varying concentrations of inhibitor were next added and pre-incubated at 25 °C for 1 h. The reaction was initiated by the addition of the fluorogenic peptide substrate Pyr-RTKR-AMC (Bachem, Switzerland) to make a final concentration of 20 μM. The reaction components were shaken for 5 s and the reaction progress monitored at 37 °C by measuring the increase in fluorescence ($\lambda_{ex}$355 nm and $\lambda_{em}$460 nm) every 45 s for 1 h on a SpectraMax Gemini XS plate reader (USA). Experiments were conducted in duplicates. $IC_{50}$ values were derived by fitting the initial velocity against the log [inhibitor] with a sigmoidal dose response curve using GraphPad Prism 5 software (USA). Nona-D-Arg-$NH_2$ peptide (GenScript, USA) was used as positive control.

### 4.3. Molecular modeling and visualization software

The WNV protease X-ray structure PDB entry 3E90 [16] was downloaded from the Protein Data Bank [www.pdb.org] and prepared with the protein preparation wizard in Maestro 9.3 (Schrödinger, USA) using standard settings. This included the addition of hydrogen atoms, bond assignments, removal of water molecules >7 Å from the ligand, protonation state assignment, optimization of the hydrogen bond network and restrained minimization using the OPLS2005 force field [22]. The co-crystallized, covalently-bound inhibitor was used as a template for modeling the conformation and orientation in the binding site of the agmatine inhibitors. The inhibitor–protein complex was finally energy-minimized using Macromodel 9.9 (Schrödinger, USA). All residues >7 Å from the ligand were constrained before the complex was subjected to 500 steps of Polak-Ribière Conjugate Gradient [23] energy minimization using the OPLS2005 force field and GB/SA continuum solvation method [24]. Model visualization was done using Chem3D Ultra v.10 software (ChembridgeSoft, USA).

## Acknowledgements

We thank A*STAR Biomedical Research Council for financial support, Dr. Manfred Raida for mass spectrometric support, Dr. Thomas Keller and Dr. Michael Entzeroth for critical reading of the manuscript.

## Appendix A. Supplementary data

Supplementary data related to this article can be found at http://dx.doi.org/10.1016/j.ejmech.2012.12.043.

## References

[1] T. Solomon, N. Engl. J. Med. 351 (2004) 370–378.
[2] L.H. Gould, E. Fikrig, J. Clin. Invest. 113 (2004) 1102–1107.
[3] L.D. Kramer, J. Li, P.-Y. Shi, Lancet Neurol. 6 (2007) 171–181.
[4] R.T. Johnson, Curr. Clin. Top. Infect. Dis. 22 (2002) 52–60.
[5] www.cdc.gov/ncidod/dvbid/westnile/index.htm.
[6] J. Kaiser, Science 337 (2012) 1030.

[7] M.S. Diamond, Antiviral Res. 83 (2009) 214–227.
[8] S. Mukhopadhyay, R.J. Kuhn, M.G. Rossmann, Nat. Rev. Microbiol. 3 (2005) 13–22.
[9] I. Radichev, S.A. Shiryaev, A.E. Aleshin, B.I. Ratnikov, J.W. Smith, R.C. Liddington, A.Y. Strongin, J. Gen. Virol. 89 (2008) 636–641.
[10] T.A. Nall, K.J. Chappell, M.J. Stoermer, N.X. Fang, J.D. Tyndall, P.R. Young, D.P. Fairlie, J. Biol. Chem. 279 (2004) 48535–48542.
[11] I. Schechter, A. Berger, Biochem. Biophys. Res. Commun. 27 (1967) 157–162.
[12] K.J. Chappell, M.J. Stoermer, D.P. Fairlie, P.R. Young, J. Biol. Chem. 281 (2006) 38448–38458.
[13] K.J. Chappell, M.J. Stoermer, D.P. Fairlie, P.R. Young, Curr. Med. Chem. 281 (2008) 2771–2784.
[14] C.G. Noble, Y.-L. Chen, H. Dong, F. Gu, S.P. Lim, W. Schul, Q.-Y. Wang, P.-Y. Shi, Antiviral Res. 85 (2010) 451–462.
[15] M.J. Stoermer, K.J. Chappell, S. Liebscher, C.M. Jensen, C.H. Gan, P.K. Gupta, W.-J. Xu, P.R. Young, D.P. Fairlie, J. Med. Chem. 51 (2008) 5714–5721.
[16] G. Robin, K. Chappell, M.J. Stoermer, S.-H. Hu, P.R. Young, D.P. Fairlie, J.L. Martin, J. Mol. Biol. 385 (2009) 1568–1577.
[17] H.A. Lim, J. Joy, J. Hill, C.S.B. Chia, Eur. J. Med. Chem. 46 (2011) 3130–3134.
[18] M.R. Wiley, N.Y. Chirgadze, D.K. Clawson, T.J. Craft, D.S. Gifford-Moore, N.D. Jones, J.L. Olkowski, A.L. Schacht, L.C. Weir, G.F. Smith, Bioorg. Med. Chem. Lett. 5 (1995) 2835–2840.
[19] G.L. Becker, F. Sielaff, M.E. Than, I. Lindberg, S. Routhier, R. Day, Y. Lu, W. Garten, T. Steinmetzer, J. Med. Chem. 53 (2010) 1067–1075.
[20] M.J.Y. Ang, H.A. Lim, C.S.B. Chia, Tetrahedron Lett. 53 (2012) 5511–5514.
[21] J.E. Knox, N.L. Ma, Z. Yin, S.J. Patel, W.-L. Wang, W.-L. Chan, K.R.R. Rao, G. Wang, X. Ngew, V. Patel, D. Beer, S.P. Lim, S.G. Vasudevan, T.H. Keller, J. Med. Chem. 49 (2006) 6585–6590.
[22] G.A. Kaminski, R.A. Friesner, J. Tirado-Rives, W.L. Jorgensen, J. Phys. Chem. B 105 (2001) 6474–6487.
[23] E. Polak, G. Ribière, Revenue Francaise informat. Recherche opérationelle, Série Rouge 16 (1969) 35–43.
[24] W. Hasel, T.F. Hendrickson, W.C. Still, Tetrahedron Comput. Methodol. 1 (1988) 103–116.